Letter

Distributed Optimal Formation Control for Unmanned Surface Vessels by a Regularized Game-Based Approach

Jun Shi and Maojiao Ye, *Senior Member, IEEE*

Dear Editor,

This letter explores optimal formation control for a network of unmanned surface vessels (USVs). By designing an individual objective function for each USV, the optimal formation problem is transformed into a noncooperative game. Under this game theoretic framework, the optimal formation is achieved by seeking the Nash equilibrium of the regularized game. A modular structure consisting of a distributed Nash equilibrium seeker and a regulator is proposed, which is theoretically shown to be effective to steer USVs towards the optimal formation. A numerical simulation example is provided to demonstrate the effectiveness of the proposed method.

Introduction: As effective tools for search, detection, navigation, rescue, and anti-terrorism attacks in sea areas, USVs are playing essential roles in maritime defense and security [1]. Many countries have been making great efforts to the development of USV-related techniques, among which formation control is one of the core focuses. Aiming at steering USVs to achieve and maintain desired shapes, formation control of USVs has received considerable attention in the past two decades [2]–[4]. For example, an USV formation control strategy under actuator saturation and unknown nonlinearities was developed [2]. Moreover, fixed-time [3] and prescribed-time [4] issues were also addressed. By noticing that in practical situations, USVs may be involved in multiple tasks, e.g., when USVs are engaged in secure escort of an important ship, they may need to form a desired shape and avoid interceptions at the same time. Thus, optimal formation control, which allows USVs to solve the global optimization problem while maintaining the desired formation shape, may be beneficial to such cases [5].

Distributed optimal formation has received some attention in recent years. Based on a distributed optimization approach, time-varying optimal formation with quadratic global objective function was considered [6]. Optimal formation with collision avoidance was addressed in [7] and predefined-time leaderless optimal formation was investigated in [8]. However, these strategies are not designed for USVs. Inspired by the widespread applications of USVs, this letter focuses on the design of distributed optimal formation control strategies for USVs by using game theory. Though, a game-based formation strategy was studied in [9] for USVs, it is worth pointing out that the "optimal" issue was not considered and only a trade-off between formation and target tracking can be achieved.

Based on the above observations, the purpose of this letter is to construct a distributed optimal formation strategy for USVs, contributing to the community in the following aspects: 1) Different from [9], an optimal formation control problem for multiple USVs is presented, in which the USVs not only need to form a predefined shape but also solve a global optimization problem. A regularized game mapping is given for the formulated optimal formation problem, which is transferred to an optimal Nash equilibrium seeking problem. By leveraging techniques from regularization, the USVs are led to the "optimal direction", which can hardly be achieved by existing results. 2) A distributed Nash equilibrium seeking strategy is proposed to solve the optimal formation game for USVs. This strategy is constructed by a modular framework of a state regulator and a Nash equilibrium seeker, which is designed by regularized gradient search and consensus protocols. 3) It is shown theoretically that the proposed seeking strategy is effective to achieve formation of USVs while solving the global optimization problem.

Corresponding author: Maojiao Ye.

Citation: J. Shi and M. Ye, "Distributed optimal formation control for unmanned surface vessels by a regularized game-based approach," *IEEE/CAA J. Autom. Sinica*, vol. 11, no. 1, pp. 276–278, Jan. 2024.

The authors are with the School of Automation, Nanjing University of Science and Technology, Nanjing 210094, China (e-mail: juns@njust.edu.cn; ye0003ao@e.ntu.edu.sg).

Color versions of one or more of the figures in this paper are available online at http://ieeexplore.ieee.org.

Digital Object Identifier 10.1109/JAS.2023.123930

Problem statement: Consider a network of N USVs, whose dynamics are described by

$$\begin{aligned}\dot{\eta}_i &= R(\psi_i)\nu_i\\ M_i\dot{\nu}_i &= -C_i(\nu_i)\nu_i - D_i\nu_i + \tau_i\end{aligned}\tag{1}$$

where $\eta_i = [x_i, y_i, \psi_i]^T \in \mathbb{R}^3$, (x_i, y_i) is the position of ith USV and ψ_i is the yaw angle of the ith USV in the earth-fixed frame. Moreover, $\nu_i = [u_i, v_i, r_i]^T \in \mathbb{R}^3$ is the velocity vector of USV i, in which u_i, v_i, and r_i denote surge, sway, and yaw velocities of the ith USV in the body-fixed frame, respectively, and $\tau_i = [\tau_{u_i}, \tau_{v_i}, \tau_{r_i}]^T \in \mathbb{R}^3$ is the control input vector. The matrices $R(\psi_i)$, M_i, $C_i(\nu_i)$, and D_i of (1) are given by [10]

$$R(\psi_i) = \begin{bmatrix}\cos\psi_i & -\sin\psi_i & 0\\ \sin\psi_i & \cos\psi_i & 0\\ 0 & 0 & 1\end{bmatrix},\ M_i = \begin{bmatrix}m_{11}^i & 0 & 0\\ 0 & m_{22}^i & 0\\ 0 & 0 & m_{33}^i\end{bmatrix}$$

$$C_i(\nu_i) = \begin{bmatrix}0 & 0 & -m_{22}^i v_i\\ 0 & 0 & m_{11}^i u_i\\ m_{22}^i v_i & -m_{11}^i u_i & 0\end{bmatrix},\ D_i = \begin{bmatrix}d_{11}^i & 0 & 0\\ 0 & d_{22}^i & 0\\ 0 & 0 & d_{33}^i\end{bmatrix}$$

where $m_{jj}^i > 0$ and $d_{jj}^i > 0$, for $i \in \mathcal{V}$, $j = 1,2,3$. Note that the matrix $R(\psi_i)$ has the following properties: 1) $R(\psi_i)^T R(\psi_i) = R(\psi_i)R(\psi_i)^T = I_3$; 2) $R(\psi_i)^T \dot{R}(\psi_i) = \begin{bmatrix}0 & -r_i & 0\\ r_i & 0 & 0\\ 0 & 0 & 0\end{bmatrix}$.

Suppose that the USVs are involved in the following optimization problem:

$$\min_{\eta\in\mathcal{S}}\ \mathcal{J}(\eta) = \sum_{i=1}^N \mathcal{J}_i(\eta_i)\tag{2}$$

where $\mathcal{J}_i(\eta_i)$ is the local objective function of USV i and $\eta = [\eta_1^T, \ldots, \eta_N^T]^T$. Moreover,

$$\mathcal{S} = \{\eta \in \mathbb{R}^{3N} | (\eta_i - e_i) - (\eta_j - e_j) = \mathbf{0}_3\}\tag{3}$$

where $e_i \in \mathbb{R}^3$ is the desired position and orientation configuration of USV i. The optimization problem (2), which is more general than that in [5] (see also the references therein), represents USVs' intention to achieve a global task such as source seeking. The constraint set (3) aims to achieve formation of the USVs. With (2) included, we term this problem as an optimal formation control problem in this letter. This letter aims to propose distributed control laws τ_i to achieve distributed optimal formation for USVs. To achieve this goal, it is supposed that the USVs are equipped with a directed graph $\mathcal{G} = \{\mathcal{V}, \mathcal{E}\}$, in which $\mathcal{V} = \{1, 2, \ldots, N\}$ represents the set of USVs and $\mathcal{E} \subseteq \mathcal{V}\times\mathcal{V}$ represents the set of edges. Moreover, the details on graph theory can be found in [11]. To further facilitate the analysis, we make the following assumptions.

Assumption 1: The communication graph $\mathcal{G}$ is directed and strongly connected.

Assumption 2: The global objective function $\mathcal{J}(\eta)$ is continuous differentiable and strongly convex in η with constant q.

Main results: This section designs a game to achieve optimal formation control of USVs. To achieve this goal, we define

$$\min_{\eta_i\in\mathbb{R}^3}\ U_i(\eta_i, \eta_{-i}) + \kappa(t)\mathcal{J}_i(\eta_i),\ \ i \in \mathcal{V}.\tag{4}$$

Here, $\kappa(t) > 0$ is a bounded, time-varying, continuous differentiable, and monotonically decreasing regularization parameter to be further determined and $U_i(\eta_i, \eta_{-i})$ is defined as

$$U_i(\eta_i, \eta_{-i}) = \frac{1}{2}\sum_{i=1}^N b_{ij}\|(\eta_i - e_i) - (\eta_j - e_j)\|^2,\ \ i \in \mathcal{V}\tag{5}$$

in which $\eta_{-i} = [\eta_1^T, \ldots, \eta_{i-1}^T, \eta_{i+1}^T, \ldots, \eta_N^T]^T$ and $b_{ij} \geq 0$ is a constant.

Remark 1: As each USV's objective function may be dependent on all USVs' positions, it is assumed that there is a graph among all

USVs. The strong connectivity of this graph by Assumption 1 ensures that each USV is able to disseminate its position information to others, by which formation can be achieved in a distributed manner.

The objective function (4) can be split into two parts. The first term $U_i(\eta_i,\eta_{-i})$ corresponds to the formation of a desired shape. The second term $\kappa(t)\mathcal{J}_i(\eta_i)$ aims to steer the Nash equilibrium of the formation game towards the minimum of the global objective function. Note that,

$$[\nabla_i U_i(\eta_i,\eta_{-i})]_{vec} = (\Xi\otimes I_3)(\eta-\mathbf{e}) \tag{6}$$

where $\Xi = \begin{bmatrix} \sum_{j=2}^{N} b_{1j} & -b_{12} & \cdots & -b_{1N} \\ -b_{21} & \sum_{j=1,j\neq 2}^{N} b_{2j} & \cdots & -b_{2N} \\ \vdots & \vdots & \ddots & \vdots \\ -b_{N1} & -b_{N2} & \cdots & \sum_{j=1,j\neq N}^{N} b_{Nj} \end{bmatrix}$, $\nabla_i U_i(\eta_i,\eta_{-i}) = \frac{\partial U_i(\eta_i,\eta_{-i})}{\partial \eta_i}$, $[\nabla_i U_i(\eta_i,\eta_{-i})]_{vec} = [\nabla_1^T U_1(\eta_1,\eta_{-1}),\ldots,\nabla_N^T U_N(\eta_N,\eta_{-N})]^T$, and $\mathbf{e} = [e_1^T,\ldots,e_N^T]^T$. Thus, the physical interactions among USVs can be modeled by Ξ, which can be seen as the Laplacian matrix of a graph. For clarity, we term this graph as interference graph [12].

Assumption 3: The interference graph is undirected and connected.

Based on Assumption 3, it is clear that $\mathcal{Q} = \{\eta|\nabla_i U_i(\eta_i,\eta_{-i}) = \mathbf{0}_3, \forall i\in\mathcal{V}\}$, which corresponds to the formation set $\mathcal{S}$, is non-empty. Taking the partial derivative of objective function (4) with respect to η_i for all $i\in\mathcal{V}$ gives the following game mapping:

$$\mathbf{U}_\kappa(\eta) = (\Xi\otimes I_3)(\eta-\mathbf{e}) + \kappa(t)\nabla\mathcal{J}(\eta) \tag{7}$$

where $\nabla\mathcal{J}(\eta) = [\nabla_1^T\mathcal{J}_1(\eta),\ldots,\nabla_N^T\mathcal{J}_N(\eta_N)]^T$ and $\nabla_i\mathcal{J}_i(\eta_i) = \frac{\partial\mathcal{J}_i(\eta_i)}{\partial\eta_i}$. Based on the definition of $U_i(\eta_i,\eta_{-i})$ and Assumption 2, it can be easily obtained that $\mathbf{U}_\kappa(\eta)$ satisfies $(\mathbf{U}_\kappa(\eta)-\mathbf{U}_\kappa(\eta^d))^T(\eta-\eta^d) \geq \kappa(t)q\,\|\eta-\eta^d\|^2$, where η, $\eta^d\in\mathbb{R}^{3N}$ for each $t\geq 0$. Therefore, the Nash equilibrium of game corresponding to (4), denoted by η_t^*, is unique. Moreover, $\mathbf{U}_\kappa(\eta_t^*) = \mathbf{0}_{3N}$.

Let $\eta^*\in\mathcal{Q}$ be the solution to

$$\min_{\eta\in\mathcal{Q}} \sum_{i=1}^{N}\mathcal{J}_i(\eta_i),\ i\in\mathcal{V}. \tag{8}$$

Then, motivated by [13], the following lemma can reveal the relationship between η_t^* and η^*.

Lemma 1: Under Assumptions 2 and 3, 1) $\lim_{t\to\infty}\eta_t^* = \eta^*$; 2) $\dot\eta_t^*$ exists almost everywhere and there exists a positive constant M_p such that $\|\dot\eta_t^*\| \overset{a.e.}{\leq} M_p\frac{|\dot\kappa(t)|}{\kappa(t)}$, if $\lim_{t\to\infty}\kappa(t) = 0$.

Remark 2: This letter transforms the optimal formation control problem (2) and (3) to a game (4) by adopting regularization techniques. Based on this idea, $\kappa(t)$ can be viewed as a regularization parameter and $\kappa(t)\mathcal{J}_i(\eta_i)$ drives the USVs to the minimization solution of (2). To be more specific, Lemma 1 demonstrates that with $\lim_{t\to\infty}\kappa(t) = 0$, the Nash equilibrium corresponding to (4) converges to the optimal formation. Therefore, one can seek the Nash equilibrium of (4) instead to achieve the optimal formation.

Based on this observation and the modular framework in [11], the control input τ_i of each USV i can be designed as

$$\begin{aligned}\tau_i = {} & C_i(\nu_i)\nu_i + D_i\nu_i - M_iR(\psi_i)^T \\ & \times(-(\eta_i - z_i) - R(\psi_i)\nu_i) - M_iR(\psi_i)^T\dot R(\psi_i)\nu_i \end{aligned} \tag{9a}$$

$$\dot z_i = -\nabla_i U_i(\mathbf{p}_i) - \kappa(t)\nabla_i\mathcal{J}_i(z_i) \tag{9b}$$

$$\dot p_{ij} = -\vartheta(t)\Big(\sum_{k=1}^{N} a_{ik}(p_{ij}-p_{kj}) + a_{ij}(p_{ij}-z_j)\Big) \tag{9c}$$

for $i\in\mathcal{V}$, where $z_i\in\mathbb{R}^3$ is an auxiliary column vector, which can be seen as the virtual position and orientation vector of USV i, $\mathbf{p}_i = [p_{i1}^T,\ldots,p_{iN}^T]^T$, p_{ij} is USV i's estimate on USV j's z_j, $\nabla_i U_i(\mathbf{p}_i) = \nabla_i U_i(\eta_i,\eta_{-i})|_{\eta=\mathbf{p}_i}$ and $\vartheta(t)$ is a time-varying, and positive parameter to be further determined. In addition, a_{ij} is the weight on each edge $(j,i)\in\mathcal{E}$.

By (1) and (9), it can be obtained that

$$\dot\eta = R(\psi)\nu \tag{10a}$$

$$\dot\nu = R(\psi)^T(-(\eta-z) - R(\psi)\nu) - R(\psi)^T\dot R(\psi)\nu \tag{10b}$$

$$\dot{\mathbf{z}} = -[\nabla_i U_i(\mathbf{p}_i)]_{vec} - \kappa(t)\nabla\mathcal{J}(\mathbf{z}) \tag{10c}$$

$$\dot{\mathbf{p}} = -\vartheta(t)(\mathcal{L}\otimes I_{3N} + B_0)(\mathbf{p} - \mathbf{1}_N\otimes\mathbf{z}) \tag{10d}$$

where $R(\psi) = \mathrm{diag}\{R(\psi_i)\}_{i\in\mathcal{V}}$ is a block diagonal matrix whose diagonal blocks are $R(\psi_i)$, $\nu = [\nu_1^T,\ldots,\nu_N^T]^T$, $\mathbf{z} = [z_1^T,\ldots,z_N^T]^T$, $\mathbf{p} = [\mathbf{p}_1^T,\ldots,\mathbf{p}_N^T]^T$, $\mathcal{L}$ is the Laplacian matrix of graph $\mathcal{G}$, $B_0 = \mathrm{diag}\{a_{ij}\otimes I_3\}_{i\in\mathcal{V}}$, and $\otimes$ represents the Kronecker product. In addition, there exists a symmetric positive definite matrix $\mathcal{P}$ such that $\mathcal{P}(\mathcal{L}\otimes I_{3N} + B_0) + (\mathcal{L}\otimes I_{3N} + B_0)^T\mathcal{P} = \mathcal{Q}$ and $\mathcal{Q}$ is a symmetric positive definite matrix by Assumption 1 [14].

Then, the following result can be derived for the optimal formation protocol (9).

Theorem 1: Under Assumptions 1–3, the optimal formation can be achieved, i.e., $\lim_{t\to\infty}\eta(t) = \eta^*$, $\lim_{t\to\infty}\mathbf{z}(t) = \eta^*$, $\lim_{t\to\infty}R(\psi_i(t))\,\nu_i(t) = \mathbf{0}_3$, and $\lim_{t\to\infty}\mathbf{p}(t) = \mathbf{1}_N\otimes\eta^*$ with $\kappa(t)$ and $\vartheta(t)$ satisfying

$$\lim_{t\to\infty}\kappa(t) = 0,\ \lim_{t\to\infty}\int_0^t\kappa(s)ds = \infty,\ \lim_{t\to\infty}\frac{|\dot\kappa(t)|}{\kappa^2(t)} = 0 \tag{11}$$

$$\kappa(t)\lambda_{\min}(\mathcal{Q})\vartheta(t) \geq \xi(\kappa) \tag{12}$$

where $\xi(\kappa) = \frac{\epsilon_1(\max_{i\in\mathcal{V}}\{l_i\})^2}{2q} + 2\kappa(t)\sqrt{N}\|\mathcal{P}\|\max_{i\in\mathcal{V}}\{l_i\} - \frac{2N\|\mathcal{P}\|^2(\sqrt{N}\max_{i\in\mathcal{V}}\{l_i\}+\kappa(t)q)^2}{q} + \kappa^2(t)\bar\iota$, $\bar\iota = q(\frac{1}{2}-\frac{1}{2\epsilon_1})$, $l_i = \sqrt{\sum_{j=1,j\neq i}^{N}(b_{ij})^2 + (\sum_{j=1,j\neq i}^{N} b_{ij})^2}$, and $\epsilon_1 > 1$ is a constant.

Proof: Let $\bar{\mathbf{z}} = \mathbf{z} - \eta_t^*$, $\bar{\mathbf{p}} = \mathbf{p} - \mathbf{1}_N\otimes\mathbf{z}$, and $V_z = \frac{1}{2}\|\mathbf{z}-\eta_t^*\|^2 + \bar{\mathbf{p}}^T\mathcal{P}\bar{\mathbf{p}}$. Then, taking the time derivatives of V_z, one has

$$\begin{aligned}\dot V_z \overset{a.e.}{=} {} & (\mathbf{z}-\eta_t^*)^T(-[\nabla_i U_i(\mathbf{y}_i)]_{vec} - \kappa(t)\nabla\mathcal{J}(\mathbf{z}) - \dot\eta_t^*) \\ & - \vartheta(t)\bar{\mathbf{p}}^T\mathcal{Q}\bar{\mathbf{p}} + 2\bar{\mathbf{p}}^T\mathcal{P}\Big(\mathbf{1}_N\otimes([\nabla_i U_i(\mathbf{p}_i)]_{vec} + \kappa(t)\nabla\mathcal{J}(\mathbf{z}))\Big) \\ \overset{a.e.}{\leq} {} & -\kappa(t)\bar\iota\|\mathbf{z}-\eta_t^*\|^2 - \Pi(\vartheta,\kappa)\|\bar{\mathbf{p}}\|^2 + \|\mathbf{z}-\eta_t^*\|\|\dot\eta_t^*\| \end{aligned} \tag{13}$$

where $\Pi(\vartheta,\kappa) = \vartheta(t)\lambda_{\min}(\mathcal{Q}) - \frac{\epsilon_1(\max_{i\in\mathcal{V}}\{l_i\})^2}{2q\kappa(t)} - 2\sqrt{N}\|\mathcal{P}\|\max_{i\in\mathcal{V}}\{l_i\} - \frac{2N\|\mathcal{P}\|^2(\sqrt{N}\max_{i\in\mathcal{V}}\{l_i\}+\kappa(t)q)^2}{q\delta(t)}$. Choosing $\vartheta(t)$ such that $\Pi(\vartheta,\kappa) \geq \kappa(t)\bar\iota$, one has

$$\dot V_z \overset{a.e.}{\leq} -\frac{\kappa(t)\bar\iota}{\max\{\frac{1}{2},\lambda_{\max}(\mathcal{P})\}}V_z + \sqrt{2V_z}M_p\frac{|\dot\kappa(t)|}{\kappa(t)} \tag{14}$$

by Lemma 1, where $\max\{\frac{1}{2},\lambda_{\max}(\mathcal{P})\}$ is a maximum value comparator. Let $\Sigma = \sqrt{2V_z}$, $E(t) = \int_{s=0}^{t}\frac{\kappa(s)}{2\max\{\frac{1}{2},\lambda_{\max}(\mathcal{P})\}}\mathrm{d}s$. The rest of the proof follows [15] to show that $\lim_{t\to\infty}\mathbf{z}(t) = \eta^*$, $\lim_{t\to\infty}\mathbf{p}(t) = \mathbf{1}_N\otimes\eta^*$, and $\lim_{t\to\infty}\|\dot{\mathbf{z}}(t)\| = 0$.

Let $\bar\eta_i = \eta_i - z_i$, $\bar\nu_i = R(\psi_i)\nu_i$, $\varpi_i = [\bar\eta_i^T,\bar\nu_i^T]^T$, $C = \begin{bmatrix} 0 & 1 \\ -1 & -1 \end{bmatrix}$, and $\mathcal{B}_i = [-\dot z_i^T,\mathbf{0}_3^T]^T$, one has

$$\dot\varpi_i = (C\otimes I_3)\varpi_i + \mathcal{B}_i. \tag{15}$$

Furthermore, by treating $\mathcal{B}_i$ as the virtual control input, it follows from the fact that $C\otimes I_3$ is Hurwitz that (15) is input-to-state stable. Since $\lim_{t\to\infty}\|\dot{\mathbf{z}}(t)\| = 0$, one has $\lim_{t\to\infty}\bar\eta_i(t) = \mathbf{0}_3$ and $\lim_{t\to\infty}\bar\nu_i(t) = \mathbf{0}_3$. Thus, the conclusion is arrived. ■

Numerical example: In this section, optimal formation control for USVs will be simulated by utilizing the proposed strategy. The local objective function for each USV i is given as $\mathcal{J}_i(\eta_i) = \frac{1}{2}\Big((x_i-x^d)^2 + (y_i-y^d)^2 + (\psi_i-\psi^d)^2\Big) = \frac{1}{2}\|\eta_i-\Delta\|^2$, where $\Delta = [x^d,y^d,\psi^d]^T$ denotes the position and orientation of the target. Thus, the optimization problem is given as

$$\min_{\eta\in\mathcal{S}} \frac{1}{2}\sum_{i=1}^{N}\|\eta_i-\Delta\|^2. \tag{16}$$

It is considered that the problem involves 5 USVs, who are equipped with the communication graph $\mathcal{G}$ shown in Fig. 1(a). In the simulation, it is supposed that $\Delta = [0,0,0]^T$. Moreover, it is set that $b_{ij} = 1$, $\forall i\neq j$, $e_1 = [0,0,-\frac{\pi}{2}]^T$, $e_2 = [-2\sqrt{3},-2,0]^T$, $e_3 = [0,-4,\frac{\pi}{2}]^T$, $e_4 = [2\sqrt{3},-2,\pi]^T$, and $e_5 = [0,-2,-\pi]^T$. Thus, it can be easily computed that $\eta_1^* = [0,2,-\frac{\pi}{2}]^T$, $\eta_2^* = [-2\sqrt{3},0,0]^T$, $\eta_3^* = [0,-2,\frac{\pi}{2}]^T$,

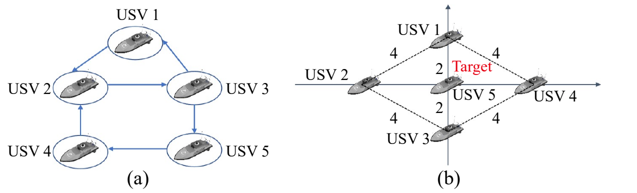

Fig. 1. Communication graph and optimal formation in the simulation. (a) The communication graph for USVs; (b) Illustration of the optimal formation for USVs.

$\eta_4^* = [2\sqrt{3}, 0, \pi]^T$, and $\eta_5^* = [0, 0, -\pi]^T$. To be more clear, the optimal formation in the simulation is illustrated in Fig. 1(b).

In the simulation, it is set that $\kappa(t) = 0.3(1+t)^{-0.5}$ and $\vartheta(t) = 25(1+t)^{0.8}$. Moreover, $\eta(0) = [1, 3, 0, -2, 1, 0, 2, 0, 0, 2, 3, 0, -2, -2, 0]$, and $\mathbf{z}$, $\mathbf{p}$, v are initialized at zero. Then, the simulation results generated by (9) are shown in Figs. 2−4. Fig. 2 plots the position trajectories of USVs, which demonstrates that the optimal formation can be achieved. The yaw angle trajectories of USVs are plotted in Fig. 3, indicating that they are all stable. Fig. 4 exhibits that the velocities of USVs converge to zero. Thus, the effectiveness of (9) is numerically confirmed.

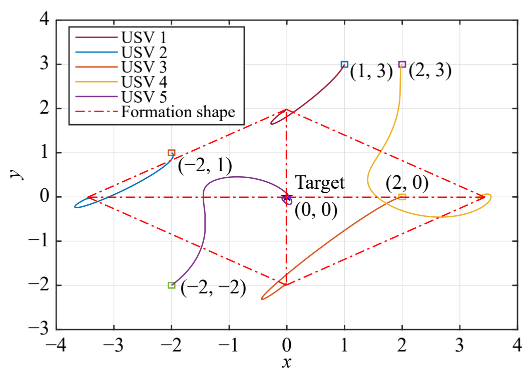

Fig. 2. The position trajectories of USVs generated by (10).

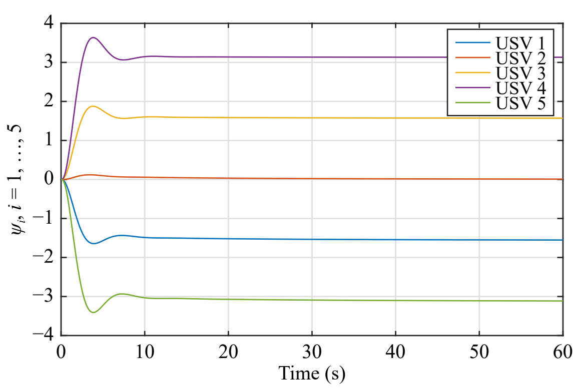

Fig. 3. The yaw angle trajectories of USVs generated by (10).

Conclusion: This letter has investigated an optimal formation control problem for multiple USVs. A game based formulation has been proposed for USVs to address this problem. Based on the formulated game, a modular framework consisting of a regulator and distributed Nash equilibrium seeker has been given to enable optimal formation for USVs. The effectiveness of the proposed method has been theoretically proven by using Lyapunov stability analysis. Future works will take collision avoidance, disturbances, and optimal formation of vehicular system (see, e.g., [16], [17]) into account.

Acknowledgments: This work was supported by the National Key R&D Program of China (2022ZD0119604), the National Natural Science Foundation of China (NSFC), (62222308, 62173181, 62221004), the Natural Science Foundation of Jiangsu Province (BK20220139), and the Young Elite Scientists Sponsorship Program by CAST (2021QNRC001).

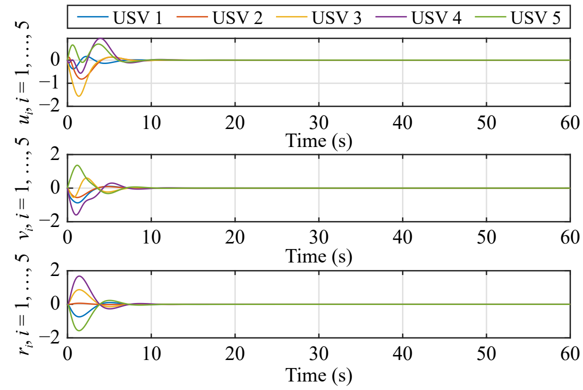

Fig. 4. The surge, sway, and yaw velocity trajectories of USVs generated by (10).

References

[1] Z. Zhou, J. Liu, and J. Yu, "A survey of underwater multi-robot systems," *IEEE/CAA J. Autom. Sinica*, vol. 9, no. 1, pp. 1–18, 2021.

[2] W. Zhou, Y. Wang, C. K. Ahn, J. Cheng, and C. Chen, "Adaptive fuzzy backstepping-based formation control of unmanned surface vehicles with unknown model nonlinearity and actuator saturation," *IEEE Trans. Vehicular Technology*, vol. 69, no. 12, pp. 14749–14764, 2020.

[3] Z. Gao and G. Guo, "Fixed-time sliding mode formation control of AUVs based on a disturbance observer," *IEEE/CAA J. Autom. Sinica*, vol. 7, no. 2, pp. 539–545, 2020.

[4] D. Rong, L. Li, and M. Tong, "Prescribed-time time-varying formation control for multiple USVs," in *Proc. Chinese Conf. Swarm Intelligence and Cooperative Control*, 2022, pp. 95–104.

[5] J. Shi, M. Ye, L. Ding, and S. Xu, "Distributed least-distance formation control for Euler-Lagrange systems: A game-based approach," *Control Engineering Practice*, vol. 142, p. 105743, 2024. DOI: 10.1016/j.conengprac.2023.105743.

[6] C. Sun, Z. Feng, and G. Hu, "Time-varying optimization-based approach for distributed formation of uncertain Euler-Lagrange systems," *IEEE Trans. Cyber.*, vol. 52, no. 7, pp. 5984–5998, 2021.

[7] L. Jiang, Z. Jin, and Z. Qin, "Distributed optimal formation for uncertain Euler-Lagrange systems with collision avoidance," *IEEE Trans. Circuits and Systems II: Express Briefs*, vol. 69, no. 8, pp. 3415–3419, 2022.

[8] P. De Villeros, J. D. Sánchez-Torres, M. Defoort, M. Djemaï, and A. Loukianov, "Predefined-time formation control for multiagent systems-based on distributed optimization," *IEEE Trans. Cyber.*, 2023, DOI: 10.1109/TCYB.2023.3264541.

[9] X. Fang, G. Wen, X. Yu, and G. Chen, "Formation control for unmanned surface vessels: A game-theoretic approach," *Asian J. Control*, vol. 24, no. 2, pp. 498–509, 2022.

[10] T. I. Fossen, *Marine Control Systems Guidance, Navigation and Control of Ships, Rigs and Underwater Vehicles*, Trondheim, Norway: Marine Cyernetics AS, 2002.

[11] M. Ye, Q.-L. Han, L. Ding, and S. Xu, "Distributed Nash equilibrium seeking in games with partial decision information: A survey," *Proc. the IEEE*, vol. 111, no. 2, pp. 140–157, 2023.

[12] M. Ye, G. Hu, F. L. Lewis, and L. Xie, "A unified strategy for solution seeking in graphical *N*-coalition noncooperative games," *IEEE Trans. Automatic Control*, vol. 64, no. 11, pp. 4645–4652, 2019.

[13] H. D. Kaushik and F. Yousefian, "A method with convergence rates for optimization problems with variational inequality constraints," *SIAM J. Optimization*, vol. 31, no. 3, pp. 2171–2198, 2021.

[14] F. L. Lewis, H. Zhang, K. Hengster-Movric, and A. Das, *Cooperative Control of Multi-Agent Systems Optimal and Adaptive Design Approaches*, London, UK: Springer-Verlag, 2014.

[15] R. I. Boţ, S.-M. Grad, D. Meier, and M. Staudigl, "Inducing strong convergence of trajectories in dynamical systems associated to monotone inclusions with composite structure," *Advances in Nonlinear Analysis*, vol. 10, no. 1, pp. 450–476, 2020.

[16] X. Ge, Q.-L. Han, X.-M. Zhang, and D. Ding, "Communication resource-efficient vehicle platooning control with various spacing policies," *IEEE/CAA J. Autom. Sinica*, 2023, DOI: 10.1109/JAS.2023.123507.

[17] X. Ge, Q.-L. Han, Q. Wu, and X.-M. Zhang, "Resilient and safe platooning control of connected automated vehicles against intermittent denial-of-service attacks," *IEEE/CAA J. Autom. Sinica*, vol. 10, no. 5, pp. 1234–1251, 2023.